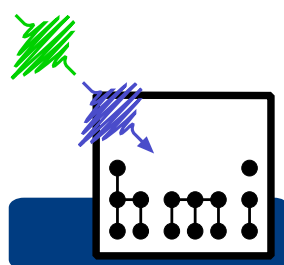


Ralph Ernstorfer

**Spectroscopic investigation of
photoinduced heterogeneous
electron transfer**



im Fachbereich Physik
der Freien Universität Berlin
eingereichte Dissertation

Berlin - Mai 2004

Abgabe der Dissertation: 27.05.2004

Tag der Disputation: 09.07.2004

Erstgutachter: Prof. Dr. Frank Willig

Zweitgutachter: Prof. Dr. Ludger Wöste

Drittgutachter: Prof. Dr. R. J. Dwayne Miller

Prof. Dr. Eberhard Riedle

Befürwortender Professor: Prof. Dr. Martin Wolf

Ralph Ernstorfer

Spectroscopic investigation of photoinduced heterogeneous electron transfer

Abstract

The dynamics of heterogeneous electron transfer are investigated by using several spectroscopic techniques. The system under study is the perylene chromophore chemically linked via different bridge-anchor groups onto the surface of nano-structured TiO₂ anatase. The energetics of the interface are characterized by UPS and XPS, revealing the molecular donor level at around 800 meV above the minimum of the conduction band of the solid. In this regime, the electron injection kinetics directly reflect the interfacial electronic coupling. The kinetics of the forward and the backward interfacial electron transfer are studied by pump-probe spectroscopy. The electron injection from perylene directly bound to the surface with a carboxylic group occurs with a time constant of 13 fs. The exchange of the anchor group by a phosphonic acid as well as the insertion of electronically saturated (sp³-hybridized) molecular units in-between the chromophore and the anchor groups systematically decelerates the electron injection. The insertion of a rigid 1 nm long molecular "tripod" stretches the electron transfer kinetics into the picosecond range. Fast (slow) electron injection is followed by fast (slow) recombination. A specific conjugated bridge is found to function as a "molecular wire" with respect to electron injection but as an sp³-hybridized analog with respect to recombination. The observed differences in the injection times for different bridge-anchor groups can be explained in terms of the molecular structures. The excited state wave functions of the isolated dyes, obtained by semi-empirical calculations, can predict qualitative trends for the interfacial electronic interaction and thus for the injection time. A rate equation model is applied for the extraction of the time constants. The validity of this model for the extraction of population kinetics on the time scale of electronic dephasing processes is verified by comparison with an adequate optical Bloch equations model. Specific experimental achievements are firstly the construction of an ultra-high vacuum chamber, with the option of introducing high purity gases and liquids, and secondly the generation of tunable sub-20 fs laser pulses by a non-collinear optical parametric amplifier at a repetition rate of 100 kHz. In particular, sub-15 fs pulses are generated in the spectral range of the perylene absorption around 435 nm. Both molecular and semiconductor moieties are characterized by stationary absorption and emission spectroscopy, FT-IR and Raman spectroscopy, as well as time-correlated single photon counting.

Ralph Ernstorfer

Spectroscopic investigation of photoinduced heterogeneous electron transfer

Kurzzusammenfassung

Mittels verschiedener spektroskopischer Methoden wurde die Dynamik von heterogenem Elektronentransfer an dem System Perylen-TiO₂ untersucht. Der Farbstoff Perylen wurde mit verschiedenen Brücke-Anker-Gruppen an die Oberfläche von nano-strukturiertem Anatas gebunden. Die elektronische Struktur der Farbstoff-Halbleiter-Grenzfläche wurde mit UPS und XPS charakterisiert. Daraus konnte die energetische Lage des Donorniveaus der Elektronentransferreaktion zu circa 800 meV oberhalb des Leitungsbandminimums des Halbleiters bestimmt werden. In dieser Situation spiegelt die Geschwindigkeit der Elektroneninjektion direkt die elektronische Kopplung zwischen Adsorbat und Festkörper wider. Die Kinetik der Elektroneninjektion und der Rekombination wurde mit Pump-Probe-Spektroskopie untersucht. Der direkt mittels einer Carboxylgruppe an die Oberfläche gebundene Farbstoff injiziert mit einer Zeitkonstanten von 13 fs. Sowohl der Austausch dieser Ankergruppe gegen eine Phosphonatfunktion als auch das Einfügen von elektronisch gesättigten, d.h. sp³-hybridisierten, molekularen Gruppen zwischen Chromophoren und Anker verlangsamt die Elektroneninjektion systematisch. Das Einfügen einer starren, 1 nm langen Gruppe (sog. "Tripod") verlangsamt den Elektronentransfer bis in den ps-Bereich. Für die verschiedenen gesättigten Brücke-Anker-Gruppen korreliert die Geschwindigkeit der Elektroneninjektion mit der Rekombinationskinetik. Eine bestimmte konjugierte Brücke hingegen verhält sich wie ein molekularer Draht bezüglich der Injektion, jedoch wie das sp³-hybridisierte Analogon bezüglich der Rückreaktion. Die experimentell beobachteten Unterschiede in den Injektionszeiten für die verschiedenen Brücke-Anker-Gruppen können in Abhängigkeit der molekularen Eigenschaften erklärt werden. Anhand der Wellenfunktionen der angeregten Zustände, die mittels semi-empirischer Methoden berechnet wurden, lässt sich qualitativ der Trend für die elektronische Kopplung des Moleküls an die Oberfläche und somit die Injektionszeit vorhersagen. Die Pump-Probe-Signale wurden mit einem Ratenkonstanten-Modell ausgewertet. Die Zuverlässigkeit dieser Methode zur Auswertung von Reaktionen, die auf der Zeitskala der elektronischen Dephasierung ablaufen, wurde durch einen Vergleich mit den optischen Bloch-Gleichungen überprüft. Experimentelle Entwicklungen im Rahmen dieser Arbeit sind unter anderem die Konstruktion einer Ultrahochvakuum-Kammer, die das Einbringen und Entfernen einer definierten Gas- oder Flüssigkeitsumgebung erlaubt, und die Erzeugung von verstimmmbaren sub-20 fs Laserpulsen mittels eines nicht-kollinearen optisch-parametrischen Verstärkers bei einer Repetitionsrate von 100 kHz. Insbesondere

konnten damit sub-15 fs Pulse im Bereich der Grundzustandsabsorption von Perylen um 435 nm erzeugt werden. Sowohl die verschiedenen Farbstoffe als auch der Halbleiter wurden mittels stationärer Absorption, Fluoreszenzspektroskopie, FT-IR- und Raman-Spektroskopie und zeitkorrelierter Einzelphotonen Zähltechnik charakterisiert.

Contents

Publications	xiii
List of Figures	xix
List of Tables	xxi
Acronyms	xxiii
Abbreviations	xxv

1 Introduction	1
1.1 General aspects and outline of this thesis	1
1.2 Introduction to electron transfer theory	4
1.2.1 Homogeneous electron transfer	4
1.2.1.1 Non-adiabatic limit	4
1.2.1.2 Adiabatic limit	9
1.2.2 Heterogeneous electron transfer	9
1.2.2.1 Non-adiabatic limit	10
1.2.2.2 Adiabatic limit	12
1.3 State of the art and open questions	13
1.3.1 Experimental studies on heterogeneous electron transfer	13
1.3.2 Theoretical studies on heterogeneous electron transfer	15
2 Experimental setup	19
2.1 UHV chamber for gas and liquid environment	19
2.1.1 Motivation	19
2.1.2 Description of the chamber	20
2.1.3 Construction of a thin UHV window	25

2.2	Laser system	27
2.2.1	Overview	27
2.2.2	100 kHz NOPA	29
2.2.3	Generation of sub-15 fs pulses around 430 nm	32
2.2.4	Probe pulses	33
2.2.5	Autocorrelation (AC)	33
2.2.6	Cross-correlation (CC)	34
2.2.7	Data acquisition	35
3	Experimental system	37
3.1	The chromophores: derivatives of perylene	37
3.1.1	Properties of the neutral chromophores	37
3.1.1.1	Electronic properties of neutral perylene	38
3.1.1.2	Investigated perylene derivatives	40
3.1.2	Excited state lifetime of the free molecule	43
3.1.3	Properties of the oxidized chromophores	45
3.1.3.1	Electronic transitions	45
3.1.3.2	Vibrational relaxation	47
3.2	The semiconductor: TiO ₂ anatase	47
3.2.1	General properties of TiO ₂	47
3.2.2	Nano-structured anatase	48
3.2.2.1	Preparation procedure	48
3.2.2.2	Characterization of nano-structured films	49
3.2.2.3	Choice of the glass substrate	51
3.2.3	Sensitization and transfer into UHV	52
3.3	Characterization of the adsorbate-surface binding configuration: FT-IR spectroscopy	52
3.4	Energy level alignment at the surface	56
3.4.1	Introduction	56
3.4.2	Valence electronic structure: UPS	57

3.4.3	Core states: XPS	60
4	Electron transfer dynamics	63
4.1	Strong coupling case: DTB-Pe-COOH on TiO ₂	63
4.1.1	General aspects of the transient absorption measurements . .	65
4.1.1.1	Assignment of the 570 nm signal	65
4.1.1.2	Data fitting - rate equation model	65
4.1.1.3	Data fitting - optical Bloch equations	67
4.1.1.4	Data fitting - coherent contributions to the pump-probe signal	73
4.1.1.5	Determination of the system function	74
4.1.2	ET mechanism	74
4.1.2.1	Stationary absorption spectroscopy	75
4.1.2.2	Electronic structure calculation of the dye-anatase system	78
4.1.2.3	Energetics of the ET reaction	80
4.1.3	General features of pump-probe transients	84
4.1.3.1	Variation of pump spectrum and probe wavelength .	84
4.1.3.2	Photo-stability of the samples.	85
4.1.3.3	Long-term cation signal	88
4.2	Electron transfer: Dependence on the chemical nature of the anchor group	88
4.2.1	Binding modes of the anchor groups	89
4.2.2	Injection kinetics and linear absorption	91
4.2.3	MO calculations of the anchor group	93
4.3	Electron transfer: Dependence on the chemical nature of the bridge	95
4.3.1	Electronically saturated bridge units: methyl groups	95
4.3.2	Electronically unsaturated bridge: DTB-Pe-CH=CH-COOH .	98
4.3.2.1	Electron injection	98
4.3.2.2	Comparison with DFT cluster calculations	100

4.3.2.3	Early recombination	102
4.3.3	Distance dependence of electronic coupling: MO study of the perylene-bridge coupling	103
4.3.4	Long-range electron transfer: DTB-Pe-tripod	106
4.3.5	Summary - distance dependence of electron transfer	109
4.4	Further aspects of interfacial electron transfer	110
4.4.1	Recombination kinetics	110
4.4.2	Reproducibility of the measurements - Diffusion of sodium from the glass substrate	113
4.4.3	Electron injection into ZnO	117
4.4.4	Solvent effects on the electron transfer	118
5	Summary	121
A	Analytical tools	125
A.1	Details of the MO calculations	125
A.2	Details of the UPS and XPS measurements	129
A.3	Further analytical tools	131
A.3.1	Single photon counting (SPC)	131
A.3.2	Stationary absorption and emission spectroscopy	131
A.3.3	FT-IR spectroscopy	131
A.3.4	Raman spectroscopy	131
A.3.5	Transmission electron microscopy (TEM)	132
A.3.6	Scanning electron microscopy (SEM)	132
Bibliography		133
Acknowledgement	155
Curriculum vitae	157

Publications

List of papers

1. R. Ernstorfer, L. Töben, L. Gundlach, S. Felber, E. Galoppini, Q. Wei, R. Eichberger, W. Storck, C. Zimmermann, F. Willig, *Femtosecond electron injection from optically populated donor states into the conduction band of semiconductors*, Proc. SPIE Int. Soc. Opt. Eng. **5223**, 110, 2003.
2. R. Ernstorfer, L. Gundlach, S. Felber, C. Zimmermann, R. Eichberger, Q. Wei, E. Galoppini, and F. Willig, *Influence of molecular spacers on ultrafast heterogeneous electron transfer*, in: M. M. Martin, J. T. Heynes (Eds.), Femtochemistry and Femtobiology, Ultrafast Events in Molecular Science, Elsevier, 521, 2004.
3. L. Gundlach, R. Ernstorfer, C. Zimmermann, R. Eichberger, S. Felber, L. Töben, E. Galoppini, Q. Wei, and F. Willig, *Heterogeneous electron transfer probed with femtosecond two-photon photoemission spectroscopy*, in: M. M. Martin, J. T. Heynes (Eds.), Femtochemistry and Femtobiology, Ultrafast Events in Molecular Science, Elsevier, 529, 2004.
4. K. Schwarzburg, R. Ernstorfer, S. Felber, and F. Willig, *Primary and final charge separation in the nano-structured dye-sensitized electrochemical solar cell*, Coord. Chem. Rev., accepted.
5. R. Ernstorfer, L. Gundlach, C. Zimmermann, F. Willig, R. Eichberger, and E. Riedle, *Generation of sub-20 fs tunable visible pulses from a 100 kHz NOPA for measuring ultrafast heterogeneous electron transfer*, Ultrafast Optics IV, 389, 2004.
6. R. Ernstorfer, S. Felber, W. Storck, E. Galoppini, Q. Wei, and F. Willig, *Distance dependence of heterogeneous electron transfer probed in ultrahigh vacuum with femtosecond transient absorption*, Res. Chem. Intermed., in print.
7. J. Piel, E. Riedle, L. Gundlach, R. Ernstorfer, and R. Eichberger, *Tunable sub-20 fs visible pulses at 100 kHz repetition rate*, as manuscript.
8. R. Ernstorfer, L. Gundlach, S. Felber, R. Eichberger, W. Storck, and F. Willig, *Anchor group-dependent heterogeneous electron transfer from perylene to nano-structured TiO₂*, as manuscript.

9. R. Ernstorfer, L. Gundlach, S. Felber, R. Eichberger, W. Storck, F. Willig, M.J. Lundqvist, and P. Persson, *Through-bridge mediated vs. through-space mediated heterogeneous electron transfer*, in preparation.
10. R. Ernstorfer, L. Gundlach, T. Hannappel, S. Kubala, and F. Willig, in preparation.

Submitted patents

1. F. Willig, R. Ernstorfer, T. Hannappel, and S. Kubala, *Vorrichtung und Verfahren zur nasschemischen Präparation von hochreinen Festkörperoberflächen*, submitted to Deutsches Patent- und Markenamt.
2. R. Ernstorfer, *Fenster für eine Ultrahochvakuum-Kammer*, submitted to Deutsches Patent- und Markenamt.

Oral presentations

1. R. Ernstorfer, L. Gundlach, S. Felber, R. Eichberger, C. Zimmermann, W. Storck, and F. Willig, *Ultrafast molecule to semiconductor electron transfer via different anchor groups in ultra-high-vacuum*, Ultrafast Phenomena 2004, accepted.
2. R. Ernstorfer, L. Gundlach, S. Felber, P. Persson, T. Letzig, C. Zimmermann, R. Eichberger, and F. Willig, *Pump-Probe-Spectroscopy of Ultrafast Heterogeneous Electron Transfer from Perylene to colloidal TiO₂*, DPG Frühjahrstagung, 2004.
3. R. Ernstorfer, L. Gundlach, C. Zimmermann, F. Willig, R. Eichberger, and E. Riedle, *Generation of sub-20 fs tunable visible pulses from a 100 kHz NOPA for measuring ultrafast heterogeneous electron transfer*, Ultrafast Optics, 2003.
4. R. Ernstorfer, L. Gundlach, S. Felber, R. Eichberger, C. Zimmermann, W. Storck, and F. Willig, *Ultrafast electron injection into the conduction band of semiconductors*, SFB 450 workshop ACU II, 2003.
5. R. Ernstorfer, C. Zimmermann, S. Felber, L. Gundlach, W. Storck, R. Eichberger, E. Galoppini, Q. Wei, and F. Willig, *Spectroscopy of Ultrafast Heterogeneous Electron Transfer from Perylene to colloidal TiO₂*, DPG Frühjahrstagung, 2003.

Poster presentations

1. R. Ernstorfer, L. Gundlach, S. Felber, C. Zimmermann, R. Eichberger, Q. Wei, E. Galoppini, and F. Willig, *Influence of molecular spacers on ultrafast heterogeneous electron transfer*, Femtochemistry VI, 2003.

The following are publications to that I have contributed but which are not included in this thesis due to the limited extent of this contribution.

- L. Töben, L. Gundlach, T. Hannappel, R. Ernstorfer, R. Eichberger, and F. Willig, *Dynamics of electron scattering between bulk states and the C_1 surface state of InP(100)*, Appl. Phys. A **78** (2004) 239
- L. Töben, T. Hannappel, R. Eichberger, K. Möller, L. Gundlach, R. Ernstorfer, and F. Willig, *Two-photon photoemission as a probe of unoccupied and occupied surface states of InP(100)*, J. Cryst. Growth. **248C** (2003) 206.

List of Figures

1.1	Illustration of homogeneous electron transfer	5
1.2	Illustration of non-adiabatic heterogeneous ET	10
2.1	Sketch of the UHV chamber for gas and liquid environment	21
2.2	Details of the solvent chamber	24
2.3	Sketch of the thin UHV window.	26
2.4	Scheme of the laser system	27
2.5	Scheme of the single stage NOPA	29
2.6	Beam geometry within the NOPA	30
2.7	Output spectra, autocorrelation traces and tuning curve	31
2.8	Sub-15 fs pump pulse: autocorrelation and spectra	32
2.9	Experimental setup of the pump-probe experiment	33
3.1	Absorption spectra of neutral and oxidized perylene	38
3.2	$S_0(^1A_g) \rightarrow S_1(^1B_{1u})$ transition of perylene	39
3.3	Structural formulas of the investigated chromophores	41
3.4	Absorption and emission spectra of the perylene chromophore	42
3.5	Molecular orbitals of neutral DTB-Pe-COOH	43
3.6	Time-resolved fluorescence of perylene	44
3.7	Visualization of the $^2A_u \rightarrow ^2B_{3g}$ transition of perylene radical cation .	46
3.8	SEM and TEM image of nano-structured TiO ₂	49
3.9	Raman spectra of the TiO ₂ film	50
3.10	Possible binding configurations of formic acid on anatase (101)	53
3.11	FT-IR spectra of sensitized TiO ₂	55

3.12 UPS spectra of sensitized TiO ₂	58
3.13 DOS of perylene for different substituted groups	59
3.14 XPS core level spectra of un-sensitized and dye loaded TiO ₂	61
4.1 ET transfer kinetics of DTB-Pe-COOH	64
4.2 ET transfer kinetics: cation and excited state signal	64
4.3 Schematic illustration of the rate equation model	66
4.4 Schematic illustration of the 4-level system	68
4.5 Solutions of the optical Bloch equations	69
4.6 Comparison of the rate equation model with optical Bloch equations .	71
4.7 Absorption spectrum of free and adsorbed DTB-Pe-COOH	75
4.8 Fit of the absorption spectra	77
4.9 Pe-COOH adsorbed on a (TiO ₂) ₆₀ cluster	79
4.10 DFT-optimized geometries of perylene	81
4.11 Illustration of the perylene potential energy surface	83
4.12 Bleaching kinetics of pump-probe signals	86
4.13 Binding geometry of DTB-Pe-P(O)(OH) ₂ on anatase (101)	89
4.14 Electron injection kinetics in dependence on the anchor group	90
4.15 Absorption spectra of adsorbed DTB-Pe-P(O)(OH) ₂ vs. DTB-Pe-COOH	92
4.16 ET transfer dynamics through different saturated bridge-anchor groups	96
4.17 Absorption spectra of DTB-Pe-CH=CH-COOH and DTB-Pe-CH ₂ -CH ₂ -COOH in 1:1 toluene:methanol and adsorbed on TiO ₂	99
4.18 ET transfer through an unsaturated bridge	100
4.19 LUMOs of DTB-perylene carbonic, acrylic and propionic acid	101
4.20 LUMOs of oxidized DTB-perylene carbonic, acrylic and propionic acid	101
4.21 Bridge mediated electronic interaction	104
4.22 Distance dependence of electronic coupling in dependence on the chemical nature of the bridge	105
4.23 Electron injection from DTB-Pe-tripod and LUMO	107

4.24 Transient absorption spectrum of DTB-Pe-tripod and DTB-Pe-CH ₂ -CH ₂ -COOH	108
4.25 Transient absorption of adsorbed DTB-Pe-tripod at 550 nm and FFT of the oscillatory signal	109
4.26 Schematic illustration of possible recombination channels	111
4.27 Recombination kinetics of the different perylene dyes	112
4.28 Reproducibility of the transient absorption measurements	114
4.29 Absorption spectrum of DTB-Pe-COOH adsorbed on anatase films prepared on different glass substrates	115
4.30 Electron injection into ZnO	117
4.31 Influence of a solvent environment on interfacial ET for DTB-Pe-COOH on anatase	120
A.1 Molecular orbitals of cationic DTB-Pe-COOH	126
A.2 Definition of the inertial axes	126
A.3 Bi-dentate surface bonding of DTB-Pe-P(O)(OH) ₂ and DTB-Pe-COOH on anatase (101)	127
A.4 Bi-dentate surface bonding of DTB-Pe-CH ₂ -CH ₂ -COOH and DTB-Pe-CH ₂ -P(O)(OH) ₂ on anatase (101)	128

List of Tables

3.1	Fit parameter of the XPS spectra of shown in Fig. 3.14	60
4.1	Intramolecular reorganization energies and structural relaxation of perylene S_1 and D_0	82
4.2	Bridge-dependent excited state level splitting	102
A.1	Fit parameters of the XPS spectra	130

Acronyms

AC	autocorrelation
ADC	analog to digital converter
BET	Brunauer-Emmet-Teller method
BBO	β -barium borate
CBM	conduction band minimum
CC	cross-correlation
CI	configuration interaction
CT	charge transfer
DFT	density functional theory
DOS	density of states
DSSC	dye sensitized solar cell
DTB	di-tertiary-butyl
EA	electron affinity
EDC	energy distribution curve
ET	electron transfer
FT-IR	Fourier-transform infrared (spectroscopy)
FWHM	full width half maximum
GVD	group velocity dispersion
GVM	group velocity mismatch
HOMO	highest occupied molecular orbital
IR	infrared
ISC	intersystem crossing
IVR	intramolecular vibrational redistribution
LUMO	lowest unoccupied molecular orbital
MO	molecular orbital
NIR	near infrared
NOPA	non-collinear optical parametric amplification/amplifier
OBE	optical Bloch equations
OD	optical density
OPA	(collinear) optical parametric amplification/amplifier
Pe	perylene
PDOS	projected density of states
PDOS _{dye}	projected density of states on the dye
RHF	spin restricted Hartree-Fock calculation

SEM	scanning electron microscopy
SHG	second harmonic generation
SPC	single photon counting
TDDFT	time-dependent density functional theory
TEM	transmission electron microscopy
TTB	tetra-tertiary-butyl
UHF	spin unrestricted Hartree-Fock calculation
UHV	ultrahigh vacuum
UPS	ultraviolet photoelectron spectroscopy
UV	ultraviolet
VBM	valence band maximum
wlc	white-light continuum
XPS	X-ray photoelectron spectroscopy
XRD	X-ray diffraction

Abbreviations

E_{act}	activation energy
E_n	eigenvalue of state n
$E_{probe}(t)$	probe field
$E_{pump}(t)$	pump field
$\delta_{i,j}$	Kronecker δ -function
$FC_{n,n'}$	Franck–Condon factor between vibronic states n and n'
$FCWD$	Franck-Condon-weighted density of states
ΔG^0	standard Gibbs free energy
Γ	level broadening
h	Planck's constant
\hbar	$h/2\pi$
$I_{pp}^{cat}(t_d)$	time-dependent cation absorption signal
$I_{pp,seq}^{cat}(t_d)$	sequential part of the time-dependent cation absorption signal
λ	reorganization energy
$\boldsymbol{\mu}$	transition dipole
$N_{cat}(t)$	cation ground state population (rate equation model)
$N_{exc}(t)$	excited state population (rate equation model)
$P^{(3)}(t, t_d)$	3rd-order polarization
\mathbf{p}	static electric dipole
\mathbf{p}_{tot}	total electric dipole of all occupied states
\mathbf{p}_{exc}	electric dipole of the excited state
$\Psi_n(r)$	eigenfunction of state n
$\rho, \rho_{i,j}$	density matrix, single element
$\rho_{dye,n}$	projected charge density on the dye of state n
τ_{fluor}	fluorescence lifetime
τ_{inj}	injection time constant
τ_{rec}	recombination time constant
T_1	energy/population relaxation time
T_2	dephasing time
T_2^*	”pure” dephasing time
t_d	delay time